Journal of Nuclear Materials 392 (2009) 1–5

Contents lists available at ScienceDirect

Journal of Nuclear Materials

journal homepage: www.elsevier.com/locate/jnucmat

Effect of ThO_2 on ionic transport behavior of barium borosilicate glasses

R.K. Mishra [a], R. Mishra [b], C.P. Kaushik [a,*], A.K. Tyagi [b], D. Das [b], Kanwar Raj [a]

[a] Waste Management Division, Bhabha Atomic Research Centre, Trombay, Mumbai 400 085, India
[b] Chemistry Division, Bhabha Atomic Research Centre, Trombay, Mumbai 400 085, India

ARTICLE INFO

Article history:
Received 2 July 2008
Accepted 2 March 2009

ABSTRACT

The present manuscript describes preparation, characterization and study of electrical behavior of barium borosilicate glasses with varying concentrations of ThO_2, maintaining constant molar ratios of SiO_2:-B_2O_3:Na_2O:BaO for all samples. The effect of ThO_2 incorporation on the ionic conductivity of glasses was studied by ac impedance analyzer, below the glass transition temperature. The diffusion coefficient (D) of the mobile Na^+ is determined from the values of electrical conductivity and density. The activation energy for sodium ion transport has been calculated from the values of diffusion coefficients at different temperatures. The electrical properties of the modified glass have been explained on the basis of the structural as well as electrostatic factors.

1. Introduction

Thorium will be used in the blanket zone of fast breeder reactors to produce fissile ^{233}U isotope, a fuel for Advanced Heavy Water Reactors (AHWR) in India [1]. The reprocessing of Th-based spent fuel will generate high level radioactive liquid waste (HLW) containing Th as one of the main constituents other than fission products, corrosion products, actinides and added chemicals. Vitrification is considered as the best demonstrated available technology for immobilization of HLW [2]. Borosilicate glass matrix is adopted world wide to immobilize HLW [3,4]. The vitrification process in India essentially consists of metering of pre-concentrated HLW and glass forming additives in the form of slurry into the process vessel of high Ni–Cr alloy (inconel 690) located in a multi-zone induction furnace [5]. In this process, the metallic melters used for vitrification undergo temperature based deformations/corrosion and requires replacement, which is a time consuming and costly affair. Further, due to the restriction of process temperature, waste loading in the vitrified waste product is limited. On account of these limitations, the steps are being taken to switch over to advanced technologies like Joule heated ceramic melter (JHCM) and cold crucible melter (CCM) which will enable to achieve high temperature resulting into higher waste loading unlike conventional induction pot melter [6]. One of the glass formulation parameters to be used with these melters is glass resistivity, which is crucial in governing performance of the joule heater. This molten glass resistivity dictates the power supply parameters like voltage and current in case of JHCM and additionally frequency for CCM. Barium borosilicate (BBS) glass has been explored to incorporate thoria containing waste and it has been shown that 5 mol% of ThO_2 can be incorporated in BBS without any phase separation [7].

The decay of radio nuclides, immobilized in the glass matrix may lead to increase in the temperature of the glass product and may create the thermal gradient. This temperature gradient can cause the diffusion of radio nuclides in the glass matrix, which is one of the most important aspects of the waste immobilization process affecting the leaching behavior of the radio nuclides from the glass matrix. Modeling of leaching behavior of radio nuclides from the glass matrix requires data on their diffusion. To asses the long term chemical durability of the glass matrix, study of diffusion of radio nuclides present in the glass assumes significant importance.

The knowledge of conductivity of the glass melt as a function of composition is required to optimize the composition of the glass, which will be ideal for the requirements of ceramic melter and melters based on the cold crucible induction technique. However, in the absence of the conductivity data of the glass melt, the trend in ionic conductivity below melting point, as function of glass composition, will provide an insight for the development of suitable glass. Understanding the ion transport mechanism in the glass matrix is possible from the conductivity measurement at different temperatures. In addition, the electrical conductivity measurement will allow determining the diffusion coefficient of alkali ions in the glass.

In this manuscript, we report the ionic conductivity of barium borosilicate glasses by ac impedance technique and the effect of ThO_2 on the ionic conductivity of the glass. Based on the electrical conductivity and density of the glasses, diffusion coefficients of the samples have been determined. The aim of this study was to determine the activation energy of ionic diffusion in barium borosilicate

* Corresponding author. Tel.: +91 22 2559 5528; fax: +91 22 2550 5147.
E-mail address: cpk@barc.gov.in (C.P. Kaushik).

0022-3115/$ - see front matter © 2009 Elsevier B.V. All rights reserved.
doi:10.1016/j.jnucmat.2009.03.001

glasses through ac conductivity measurements, which will help to understand the effect of ThO_2 in the diffusion of sodium in these glasses.

2. Experimental

BBS glass samples were prepared by thoroughly mixing appropriate amounts of different chemicals like silica, boric acid, barium nitrate, sodium nitrate and thorium nitrate of high purity (AR Grade >99.9%) in agate mortar for 100 g batch size scale. The powdered mixtures were well grounded and transferred into a platinum crucible and heated at 700 °C for 2 h to complete the calcinations and then further heated at 1000 °C. The melt was maintained at this temperature for 5 h to ensure homogenization. The free flowing melt was poured into preheated cylindrical graphite mould of internal diameter 11 mm and length 20 mm. The glass samples in the form of rods were cut into uniform circular pellets of diameter 11 mm and thickness about 1 mm.

The compositions of glasses were selected having ThO_2 concentration ranges from 0 to 5 mol% while maintaining the SiO_2/Na_2O, SiO_2/B_2O_3, SiO_2/BaO, B_2O_3/Na_2O, B_2O_3/BaO and BaO/Na_2O ratios constant for all the glass samples (Table 1).

The amorphous nature of these glass samples were confirmed by X-ray diffraction (XRD) using a Philips X'Pert Pro diffractometer with monochromatized Cu-Kα radiation. The glass transition temperature (*Tg*) of the samples were determined by differential thermal analysis (DTA) technique using Schimadzu DT-30 instrument in argon atmosphere and at a heating rate of 10 K/min. Structural elucidation of borosilicate network of these glass samples were determined by recording ^{29}Si and ^{11}B MAS NMR patterns using a Bruker Advance DPX 300 machine. Density of the glass samples was measured following Archimedes' principle with distilled water as immersing liquid on a single pan electronic balance with an accuracy of ±0.02 g/cc.

The electrical conductivity of the glass samples in the form of pellets (11 mm diameter and 0.5–1 mm thickness) was measured by a Solatron Impedance Analyzer (Model SI 1260) in the frequency range of 1 MHz to 1 Hz and with ac voltage amplitude 100 mV and dc bias 0 mV. The impedance analyzer measures the complex impedance ($Z^* = Z' + iZ''$) of a sample as a pair of values Z' and Z'' for each of frequency *f*. The complex impedance was automatically converted into complex capacitance $C^* = C' + iC''$ by an internal algorithm according to the following formula:

$$C^* = \frac{1}{i\omega Z^*}, \tag{1}$$

where ω is the angular frequency and $\omega = 2\pi f$.

The electric modulus is given by:

$$M^* = M' + iM'' = i\omega C_o Z^*, \tag{2}$$

where C_o, the empty cell capacitance = $\varepsilon_o A/l$; *A* is sample area and *l* is the sample thickness.

Table 1
Composition and properties of glasses.

Glass	SBTh-0	SBTh-2	SBTh-4	SBTh-5
Composition (mol%)				
SiO_2	47.34	46.40	45.45	44.97
B_2O_3	26.80	26.26	25.73	25.46
Na_2O	14.30	14.01	13.73	13.59
BaO	11.56	11.33	11.09	10.98
ThO_2	0.00	2	4	5
Density (g cm^{-3})	2.96	3.10	3.23	3.30
C_{Na} ($\times 10^{21}$ cm^{-3})	6.93	6.76	6.58	6.49
T_g (K)	832	830	831	830
(E_a ± 0.01) (eV)	1.15(1)	1.13(1)	1.08(1)	1.13(3)

Each parallel *RC* element results in a semicircle in Z^* and M^* complex plane plots and in a Debye peak in spectroscopic plots of the imaginary components, Z'' and M'' versus log *f*. The Debye peak in the Z'' and M'' spectra is described by:

$$Z'' = -R\left[\frac{\omega RC}{1+(\omega RC)^2}\right], \tag{3}$$

$$M'' = \frac{C_0}{C}\left[\frac{\omega RC}{1+(\omega RC)^2}\right], \tag{4}$$

Where

$$\omega = 2\pi f_{max} = (RC)^{-1} = \tau^{-1}, \tag{5}$$

Z'' and M'' will reach the maxima which can be expressed as:

$$Z''_{max} = -\frac{R}{2}, \tag{6}$$

$$M''_{max} = -\frac{C_0}{2C}. \tag{7}$$

Hence, the magnitudes of *R* and *C* can be estimated from either Z_{max} or M_{max}, using Eqs. (5)–(7).

Each of the pellets was uniformly coated with a thin layer of silver paste to have proper electrical contact with platinum electrode. The impedance measurement was carried out under static air in the temperature range 700–820 K. The samples were equilibrated for 30 min at the set temperatures before the impedance measurements. The temperatures were maintained within ±1 K using a microprocessor. The resistances of the pellets were obtained from the real part of the Cole–Cole plot.

3. Results and discussions

Glassy nature of the samples containing up to 5 mol% of ThO_2 was confirmed by the broad XRD peak centered around $2\theta = 13°$, which is characteristic of the amorphous borosilicate network. Beyond 5 mol% incorporation of ThO_2 in glass, phase separation of ThO_2 takes place [7]. DTA patterns for four representative glass samples having 0, 2, 4 and 5 mol% of ThO_2, are shown in Fig. 1. For the glass sample without any ThO_2 (0 mol%) DTA pattern

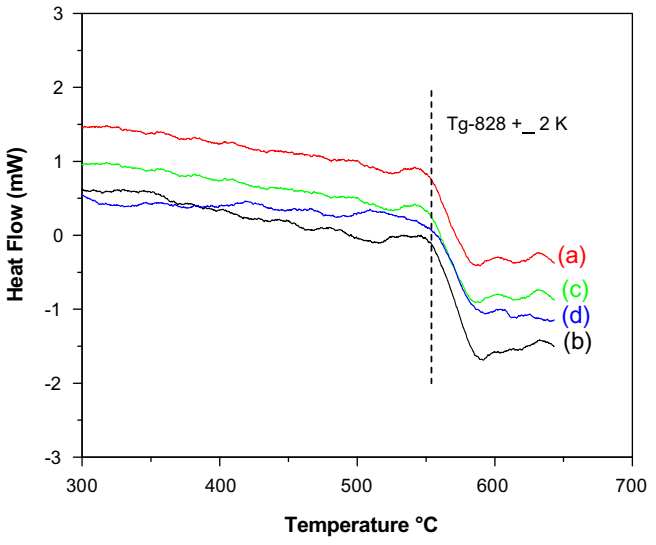

Fig. 1. DTA patterns for barium borosilicate glasses containing: (a) 0 mol%, (b) 2 mol%, (c) 4 mol% and (d) 5 mol% of ThO_2.

(Fig. 1(a)) is characterized by a broad endothermic peak centered around 850 K with an onset around 825 K. The broad endothermic peak has been attributed to the glass transition temperature (T_g). The glass transition temperature has been found to be same for all the glass samples containing different amounts of ThO_2 as can be seen from Fig. 1(a)–(d) indicating that there is no interaction between Th^{4+} ions and the borosilicate glass network. ^{29}Si MAS NMR patterns for these glasses are shown in Fig. 2. Barium borosilicate glass without any ThO_2 (0 mol%) is characterized by an asymmetric peak around −89.5 ppm. Deconvolution of this peak assuming a Guassian line shape resulted in two peaks around −95 and −86 ppm. Based on the ^{29}Si MAS NMR studies on borosilicate glasses [8–9], the peak around −95 ppm has been attributed to the Q^3 structural units of silicon and that around −86 ppm has been attributed to Q^2 structural units (where Q^n represents silicon structural units having 'n' bridging oxygen atoms). With increase in ThO_2 concentration in the glass, the line shape and peak maxima of the ^{29}Si MAS NMR patterns remained identical. This establishes the fact that the borosilicate network is unaffected by the ThO_2 incorporation in the glass.

Fig. 3 gives the electrical conductivity $\sigma(\omega)$ derived from the real part of the Cole–Cole plot versus the ac frequency for glasses containing 0, 2, 4 and 5 mol% of ThO_2 at the selected temperature of 815 K. It can be observed from the figure that the conductivity of the glass samples remains almost constant in the frequency range 1 Hz–1 MHz and increase sharply above this frequency range. The plateau value corresponds to static conductivity for long range ionic displacement, while the increase at high frequency is due to relaxation caused by local motion of Na^+ cations [10] envisaged by single ionic jump diffusion mechanism as proposed by many authors [11,12]. Fig. 3 also indicates that the increase in concentration of ThO_2 in the BBS glass samples does not change conductivity of the BBS glass samples significantly. This can be explained by the fact that the ThO_2 does not affect the borosilicate network in BBS glass, as revealed by measurement of glass transition temperature by DTA (Fig. 1) and ^{29}Si and ^{11}B MAS NMR (Fig. 2) patterns. However, the slight observed decrease in conductivity of glass samples with increase in ThO_2 concentration could be due to the net decrease in Na^+ ion concentration with increase in ThO_2 concentration.

Fig. 4 gives the Nyquist diagram ($-Z''$ versus Z') for glass containing 0, 2, 4 and 5 mol% of ThO_2 recorded at 773 K. In this diagram, a semi-circular arc centered slightly below the real axis was obtained. From the plot it can be seen that all the semicircles

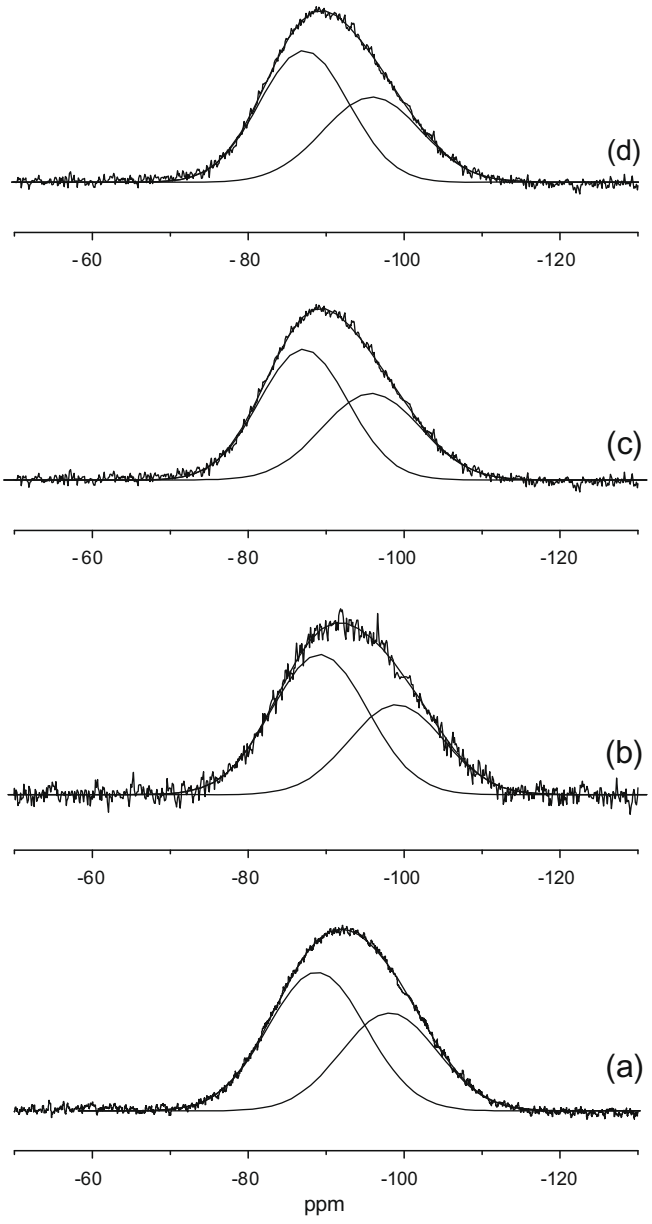

Fig. 2. ^{29}Si MAS NMR patterns for barium borosilicate glasses containing: (a) 0 mol%, (b) 2 mol%, (c) 4 mol% and (d) 5 mol% of ThO_2.

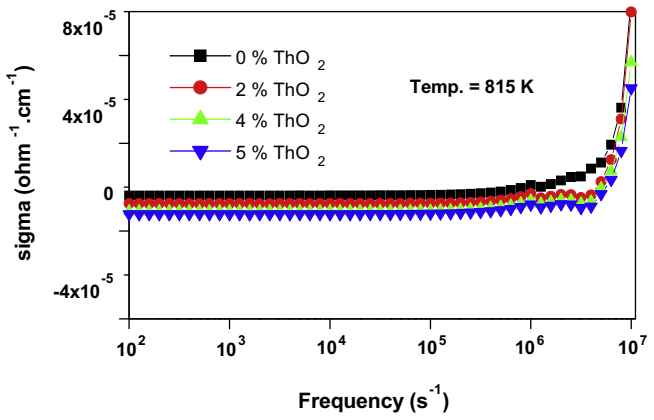

Fig. 3. Conductivity as function of frequency for glass samples at 815 K containing 0, 2, 4 and 5 mol% of ThO_2.

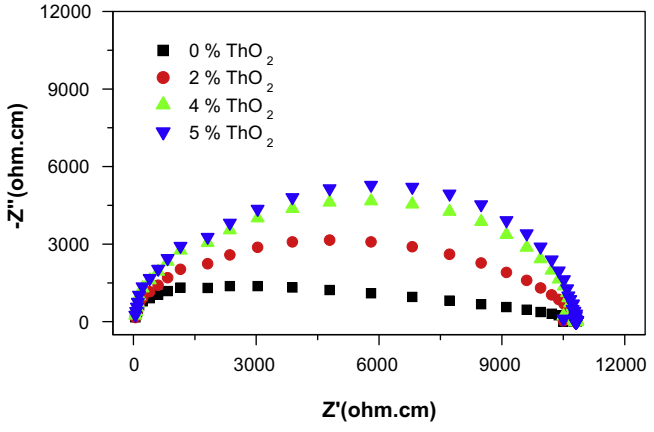

Fig. 4. Nquist plot for glass samples containing 0, 2, 4 and 5 mol% of ThO_2, measured at 773 K in the frequency range 1 Hz–10 MHz.

Table 2
Ionic conductivity for different compositions of ThO_2 at representative temperatures.

Temperature (K)	Ionic conductivity (ohm^{-1} cm^{-1})			
	0 mol% ThO_2	2 mol% ThO_2	4 mol% ThO_2	5 mol% ThO_2
710	0.009	0.012	0.010	0.008
720	0.013	0.018	0.012	
730	0.018	0.023	0.016	
740	0.025	0.028	0.021	0.020
750	0.032	0.037	0.025	0.026
775	0.048	0.055	0.037	0.036

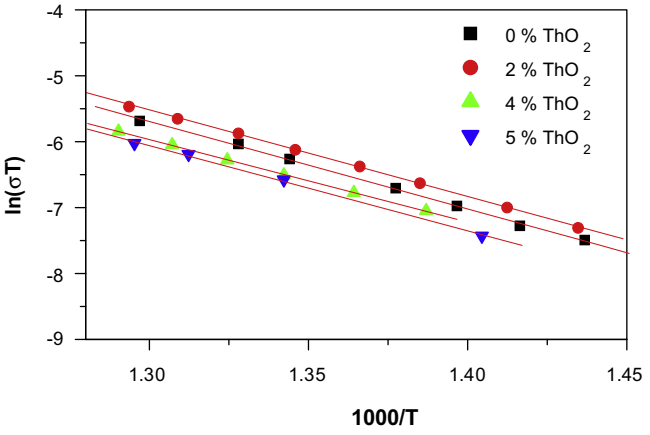

Fig. 5. Plots of $\ln(\sigma T)$ versus $1/T$ for 0, 2, 4 and 5 mol% of ThO_2.

intersect the real axis (X-axis) at same points, where as the *Y-component* of the curves increases with increase in the thorium content. The intersection of the curve with the real axis gives the resistance R_{dc} which can be related to static conductivity (σ_{dc}) given by:

$$\sigma_{dc} = \frac{1}{R_{dc}} \times \frac{l}{S}, \tag{8}$$

where l is the thickness and S is the cross sectional area of the pellet. The values of conductivity of BBS samples containing 0, 2, 4 and 5 mol% of ThO_2 at representative temperatures are given in Table 2. Fig. 5 describes the variation of conductivity $\ln(\sigma T)$ with temperature ($1/T$). The conductivity of the glass samples were found to increase with temperature, which is explained on the basis of thermally stimulated dislocation of alkali cation from its equilibrium position to an interstitial position followed by random diffusion through interstitial sites as proposed by Kelly and Tomozawa [13]. The increase in the Y-component i.e. capacitance of the glass samples with increase in the concentration of ThO_2 (Fig. 4) can be explained by the fact that the charge separation between the negatively charged borosilicate network (due to the presence of non bridging oxygen) and the large size as well as high positively charged Th^{4+} ion increased with the concentration of ThO_2.

3.1. Calculation of diffusion coefficient

The diffusion coefficient of the mobile sodium ion can be obtained by relating the electrical conductivity with the diffusion coefficient D using Nernst–Einstein equation [14]:

$$\sigma = \left(\frac{q^2}{kT}\right) \times C_{Na} \times D_{\sigma}, \tag{9}$$

where q represents the charge of the mobile ion, C_{Na} is the number of sodium atom per unit volume calculated using the relation:

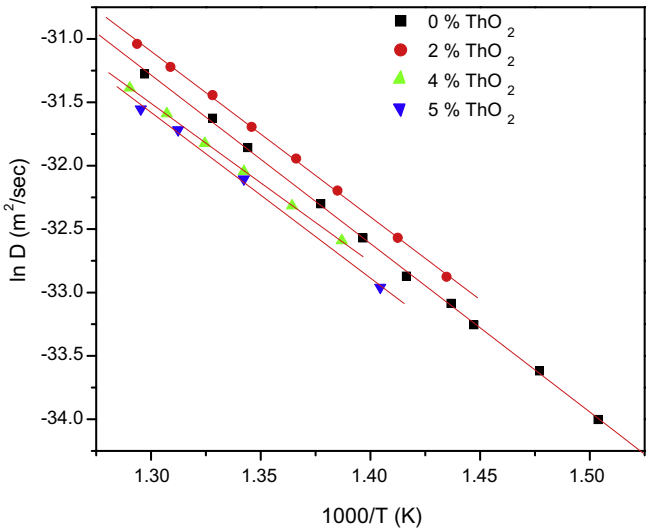

Fig. 6. Plots of $\ln(D)$ versus $1/T$ for 0, 2, 4 and 5 mol% of ThO_2 containing glasses below the glass transition temperature.

$$C_{Na} = \rho Z_{Na} N/M, \tag{10}$$

where ρ represents the sample density, Z_{Na} the number of sodium atoms in the chemical formula, N Avogadro's number, and M, the molar mass of the sample. The values of density and C_{Na} are given in Table 1. The diffusion coefficient for the transport of the charge carrier (Na^+ ion) as a function of temperature for glass samples containing different mol% of ThO_2 was calculated by using the above relation. The diffusion coefficient was found to be almost constant with ThO_2 concentration. Fig. 6 gives the plots of $\ln(D)$ versus $1/T$ below the glass transition temperature for barium containing glasses. It can be observed from these plots that all glasses have a linear plot, which is characteristic of a thermally activated transport phenomenon. The activation energy for the glass samples containing 0, 2, 4 and 5 mol% of ThO_2 calculated from the slope of theses curves are found to be 1.15(1), 1.13(1), 1.08(1) and 1.13(3) eV, respectively. The activation energy for the thermally activated transport of Na^+ ion is found to remain by and large same with ThO_2 content in the glass matrix. The constancy in activation energy with increasing ThO_2 content in the glass matrix can be explained on the fact that ThO_2 does not modify the borosilicate network, which makes the number of available sites for ionic movements constant.

4. Conclusions

The ionic conductivity of barium borosilicate glasses have been measured by ac impedance technique below the glass transition temperature. The ionic conductivity of the barium borosilicate glasses is independent of ThO_2 content up to 5 mol%. The results of electrical properties, DTA and ^{29}Si and ^{11}B MAS NMR studies suggest that borosilicate network is unaffected by the ThO_2 incorporation in the glass. The diffusion coefficients for migration of Na^+ ion have been calculated from the electrical conductivity and density data. The activation energy for ion transport calculated from the $\ln(D)$ versus $1/T$ plot for 0, 2, 4 and 5 mol% of ThO_2 was found to be 1.15(1), 1.13(1), 1.08(1) and 1.13(3) eV, respectively.

Acknowledgement

Authors thank Dr V. Sudersan for carrying out NMR studies of the glass samples.

References

[1] Anil Kakodkar, in: Proceedings of International Seminar on the Role of Nuclear Energy for Sustainable Development. New Delhi, India, 1997, p. 62.
[2] W. Lutze, R.C. Ewing (Eds.), Radioactive Waste Forms for the Future, North-Holland, Amsterdam, 1988, p. 31.
[3] L.L. Hench, D.E. Clark, J. Campbell, Nucl. Chem. Waste Manage. 5 (1984) 149.
[4] A.J. Freeman, G.H. Lander (Eds.), Handbook on the Physics and Chemistry of the Actinides, Elsevier, 1987, p. 271.
[5] K. Raj, K.K. Prasad, N.K. Bansal, Nucl. Eng. Des. 236 (2006) 914.
[6] S.D. Misra, in: Proceedings National Symposium on Science and Technology of Glass/Glass–Ceramic (NGSC-06), 2006, p. 16.
[7] R.K. Mishra, Pranesh Sengupta, C.P. Kaushik, A.K. Tyagi, G.B. Kale, Kanwar Raj, J. Nucl. Mater. 360 (2007) 43.
[8] V.K. Shrikhande, V. Sudarsan, G.P. Kothiyal, S.K. Kulshreshtha, J. Non-Cryst. Solids 283 (2001) 18.
[9] V. Sudarsan, V.K. Shrikhande, G.P. Kothiyal, S.K. Kulshreshtha, J. Phys.: Condens. Matter. 14 (2002) 6553.
[10] K. Funke, Prog. Solid State Chem. 22 (1993) 111.
[11] J.L. Souquet, M. Duclot, M. Levy, Solid State Ionics 105 (1998) 237.
[12] Arpad W. Imre, Stephan Voss, Helmut Mehrer, J. Non-Cryst. Solids 333 (2004) 231.
[13] J.E. Kelly, M. Tomozawa, J. Non-Cryst. Solids 51 (1982) 345.
[14] A. Grandjean, M. Malki, C. Simonnet, J. Non-Cryst. Sol. 352 (2006) 2731.